






Estimation of Skin Conductance Response Through Adaptive Filtering

Pietro Savazzi¹ , Floriana Vasile¹, Natascia Brondino² , Marco Vercesi²,
and Pierluigi Politi² 

¹ Department of Electrical, Computer and Biomedical Engineering,
University of Pavia, Pavia, Italy

pietro.savazzi@unipv.it, vasilefloriana@gmail.com

² Department of Brain and Behavioral Sciences, University of Pavia, Pavia, Italy

{natascia.brondino,pierluigi.politi}@unipv.it,

marco.vercesi01@universitadipavia.it

Abstract. The importance of medical wearable sensors is increasing in aiding both diagnostic and therapeutic protocols, in a wide area of health applications. Among them, the acquisition and analysis of electrodermal activity (EDA) may help in detecting seizures and different human emotional states. Nonnegative deconvolution represents an important step needed for decomposing the measured galvanic skin response (GSR) in its tonic and phasic components. In particular, the phasic component, also known as skin conductance response (SCR), is related to the sympathetic nervous system (SNS) activity, since it can be modeled as the linear convolution between the SCR driver events, modeled by sparse impulse signals, with an impulse response representing the sudomotor SNS innervation. In this paper, we propose a novel method for implementing this deconvolution by an adaptive filter, determined by solving a linear prediction problem, which results independent on the impulse response parameters, usually represented by sampling the biexponential Bateman function. The performance of the proposed approach is evaluated by using both synthetic and experimental data.

Keywords: Galvanic skin response · Electrodermal activity · Skin conductance response · Adaptive filter · Wearable sensor

1 Introduction

Galvanic skin response (GSR) may be recorded by measuring the conductance variations over a person's skin in response to sweat secretions. This electrodermal activity (EDA) is due to sweat secretion which alters the electrical property of the skin [4], in response to emotional states like arousal [13], since the GSR signal carries significant information related to neuron firing [10].

By means of modern wearable devices, like the Emaptica E4 [9] bracelet or the Affectiva Q sensor [8], it is possible measuring GSR signals during everyday

© ICST Institute for Computer Sciences, Social Informatics and Telecommunications Engineering 2019

Published by Springer Nature Switzerland AG 2019. All Rights Reserved

L. Mucchi et al. (Eds.): BODYNETS 2019, LNICST 297, pp. 206–217, 2019.

https://doi.org/10.1007/978-3-030-34833-5_17

human activities, allowing interesting medical application especially, but not only, in the field of psychiatry for aiding mental health diagnosis and therapies [12].

A GSR signal may be represented by the sum of two different components [2, 6, 7]:

- a tonic component, also known as skin conductance level (SCL), a slowly varying signal which is not caused by instantaneous external stimuli but it could be related to the level of attention;
- a phasic or skin conductance response (SCR) component which is caused by sympathetic nervous system (SNS) sporadic stimuli and it usually lasts for a few seconds.

Summarizing, while the SCL represents a measure of the complete absorption of sweat in the human' skin, SCR signals measure discrete and sporadic sweat production events driven by external stimuli caused by user's excitement or any other emotional state variation. Following this reasoning, the primary objective of EDA signal analysis is to extract the SCR components in order to firstly identifying and, in a second step, classifying the different emotional states.

The extraction of SCR events may be pursued by empirical peak detection techniques that they not take into accounts the effects of closely superimposing SCR responses. For this reason, many literature works focus on deconvolution techniques, usually taking into account nonnegative constraints and signal pre-analysis in order to jointly estimate both SCL and SCR components, see [2] and references therein.

Recently, the sparse nature of SCR signals suggests to use compressed sensing (CS) techniques to determine the driven event impulses by mean of convex optimization [6, 7], often exploiting CS reconstruction algorithm constraints for the joint estimation of the tonic and phasic signals.

Since CS reconstruction algorithms are mainly based in convex optimization analysis performed offline after the signal acquisition, in this work we are mainly interested in looking for alternative solutions that could be easily implemented in wearable devices able to provide real-time outputs. These outcomes may be useful on order to rapidly use this information for therapeutic purposes like behavioral interventions in several mental health disorders.

On this purpose, we started from more traditional deconvolution techniques by deriving an adaptive filter which is independent on the specific SCR impulse model parameters, by anyway using an optimization criterion based on the signal sparsity.

The rest of this paper is organized as follows: Sect. 2 is devoted to describe the GSR signal model used in this work, while in Sect. 3 we describe the proposed algorithm derivation. Finally, after exposing the obtained simulated and experimental data results, respectively in Sects. 4 and 5, some final concluding comments and perspective of future works end the paper.

2 EDA Signal Generation Model

2.1 Continuous-Time Model

Following the GSR signal decomposition in its tonic and phasic components, the acquired sensor signal in the continuous-time domain may be represented as:

$$y(t) = h_{ct}(t) * x(t) + b(t) + n(t) \quad (1)$$

where the phasic component is modeled as the linear convolution between the unknown sparse driver $x(t)$, corresponding to the sudomotor SNS innervation, and the impulse response $h_{ct}(t)$; $b(t)$ denotes the tonic slowly varying component, while $n(t)$ represents the electrical thermal noise contribution, modeled as additive white Gaussian noise (AWGN).

The impulse response $h_{ct}(t)$ is commonly modeled by the so called Bateman function [3, 15]:

$$h_{ct}(t) = g \left(e^{-\frac{t}{\tau_1}} - e^{-\frac{t}{\tau_2}} \right) \quad (2)$$

where g is a gain factor, while the authors of [15] used the following parameter values for all the analyzed data in their paper: $\tau_1 = 0.75$ s, and $\tau_2 = 2$ s.

2.2 Discrete-Time Model

In the following, we consider the discrete-time equivalent of Eq. (1)

$$\mathbf{y} = \mathbf{h} * \mathbf{x} + \mathbf{b} + \mathbf{n} \quad (3)$$

by taking sequences of length NT_s seconds, where N is length of \mathbf{y} in number of samples, and T_s the sampling time.

The continuous impulse response of Eq. (2) becomes

$$h(n) \equiv h_{ct}(nT_s) = g \left(e^{-\frac{nT_s}{\tau_1}} - e^{-\frac{nT_s}{\tau_2}} \right) \quad (4)$$

with $\mathbf{h} = [h(0), h(1), \dots, h(N-1)]$. Usually the EDA sensor output is sampled at a frequency $\frac{1}{T_s} \geq 4$ Hz.

3 Adaptive Filtering

3.1 Deconvolution Filter

The SCR impulse response in Eq. (4) may be represented as an infinite impulse response (IIR) linear system whose z -transform is

$$H(z) = \frac{gz^{-1}(e^{-\alpha_1} + e^{-\alpha_2})}{1 - (e^{-\alpha_1} + e^{-\alpha_2})z^{-1} + e^{-\alpha_1 - \alpha_2}z^{-2}} \quad (5)$$

where $\alpha_1 = \frac{T_s}{\tau_1}$, $\alpha_2 = \frac{T_s}{\tau_2}$.

According to Eq. (5) and initially neglecting, as usually done in the cited literature, both the tonic and noise components, the deconvolution of the EDA signal $y(n)$ can be performed by filtering each measured sequence \mathbf{y} by the following finite impulse response (FIR) filter

$$\mathbf{b} = [1, - (e^{-\alpha_1} + e^{-\alpha_2}) z^{-1}, e^{-\alpha_1 - \alpha_2} z^{-2}] \tag{6}$$

3.2 Adaptive Filter Derivation

The discrete-time difference equation corresponding to (5) can be written as

$$\beta x(n - 1) = y(n) + w(1)y(n - 1) + w(2)y(n - 2) \tag{7}$$

where

$$\begin{aligned} \beta &= g (e^{-\alpha_1} + e^{-\alpha_2}) \\ w(1) &= - (e^{-\alpha_1} + e^{-\alpha_2}) \\ w(2) &= e^{-\alpha_1 - \alpha_2} \end{aligned}$$

Since the actual shape of the impulse $h(n)$ is unknown, and the real SCR response could be generated by overlapped pulses with different time lengths, see for instance how in [6] the same problem is faced by a multiscale analysis, we may assume a filter length equal to $p + 1$ that could be greater than 3. Following this reasoning, we may define a new difference equation

$$\beta x(n - 1) = y(n) + \sum_{i=1}^p w(p)y(n - p) \tag{8}$$

In order to look for a sparse solution for $x(n)$ we may find the filter coefficients $w(k)$ which minimize

$$E \{x^2(n)\}, \tag{9}$$

by computing

$$E \left\{ \frac{\partial x^2(n - 1)}{\partial w(k)} \right\} = 0 \tag{10}$$

where E denotes the expectation operator, and $\frac{\partial}{\partial w(k)}$ the partial derivative with respect to the filter coefficient $w(k)$.

The solution of (10), using (8), is given by the following Wiener-Hopf equations [5]

$$\mathbf{w} = \mathbf{R}_y^{-1} \mathbf{r}_y \tag{11}$$

where

$$\mathbf{w} = [w(1), w(2), \dots, w(p)], \tag{12}$$

$$\mathbf{r}_y = [r_y(1), r_y(2), \dots, r_y(p)], \tag{13}$$

and

$$\mathbf{R}_y = \begin{bmatrix} r_y(0) & \cdots & r_y(p-1) \\ \vdots & \ddots & \vdots \\ r_y(p-1) & \cdots & r_y(0) \end{bmatrix} \quad (14)$$

where $r_y(k) = E\{y(n)y(n-k)\}$ is the autocorrelation of the EDA signal $y(t)$.

It is interesting to note that the constraint in (8), derived from (5), (7), and corresponding to $w(0) = 1$, actually makes the Wiener-Hopf solution equivalent to one of a linear predictor of order p .

The filter coefficients may be computed by solving Eq. (11) over a suitable time window, or, with a lower computational complexity, by the correspondent stochastic gradient solution

$$\mathbf{w}_{n+1} = \mathbf{w}_n + \mu x(n-1)\mathbf{y}_n \quad (15)$$

where \mathbf{w}_n denotes the filter coefficient vector at the discrete time instant n , $\mathbf{y}_n = [y(n), y(n-1), \dots, y(n-p)]$, and μ is a suitable step size.

Finally, the sparse impulse signal $x(n)$ may be computed by (8), while the nonnegative constraint has been taken into account by setting $x(n) = 0$ when $x(n) = m < 0$, by considering the tonic signal $b(n) = -m$.

4 Simulation Results

For synthetic data experiments, we have taken into account the generation model, described in [7], which considers a baseline component, i.e., the tonic one, inspired by the fact that wearable sensor movements may cause changes in the measured EDA signal.

Considering the discrete-time SCR signal \mathbf{x} of (3) with a length of N samples, we may assume a number of ideal pulses different from zero equal to s , which denotes the SCR driven signal sparsity. According to this premise, the SCR ideal pulses lie in the set

$$X(s, \delta) = \{\mathbf{x} | \mathbf{x} \in \mathbb{R}^N, \|\mathbf{x} - \mathbf{x}_s\|_1 \leq \delta\} \quad (16)$$

where δ is a suitable constant threshold, and \mathbf{x}_s has exactly s non zeros elements corresponding to the s largest components of \mathbf{x} . $\|\cdot\|_1$ represents the L^1 norm.

In a similar manner, it is possible to define the baseline signal \mathbf{b} to lie in the set

$$B(c, \lambda) = \{\mathbf{b} | \mathbf{b} \in \mathbb{R}^N, \|\mathbf{D}\mathbf{b} - \mathbf{D}\mathbf{b}_c\|_1 \leq \lambda\} \quad (17)$$

where c and λ have a similar meaning to respectively s and δ , and \mathbf{D} is the pairwise difference matrix defined in [7], so that $\mathbf{D}\mathbf{b}$ corresponds to the first discrete derivative of \mathbf{b} . Moreover, the parameter c denotes the number of baseline jumps due to sensor movements.

4.1 Simulation Parameters

We have considered multiple repetitions of the EDA signal \mathbf{y} with a length equal to 400 samples and the sampling frequency equal to 4 Hz, corresponding to a time duration of 100 s. The parameters λ, δ of(16), (17), have been all set to 0.01, and the added Gaussian noise corresponds to a signal-to-noise ratio of 15 dB. We have found that the value of the adaptive filter order p which gets the best simulated and experimental results is in the interval (2, 10). The following results have been obtained by setting $p = 10$.

4.2 Mean-Square Error Performance

Since we know the event signal $x(n)$, in order to assess the algorithm performance for the simulated data we may use the average mean-square error (MSE), defined as

$$\xi = \frac{E \left\{ (\mathbf{x} - \hat{\mathbf{x}})^2 \right\}}{E \left\{ \mathbf{x}^2 \right\}} \tag{18}$$

with $\hat{\mathbf{x}}$ the estimated event signal.

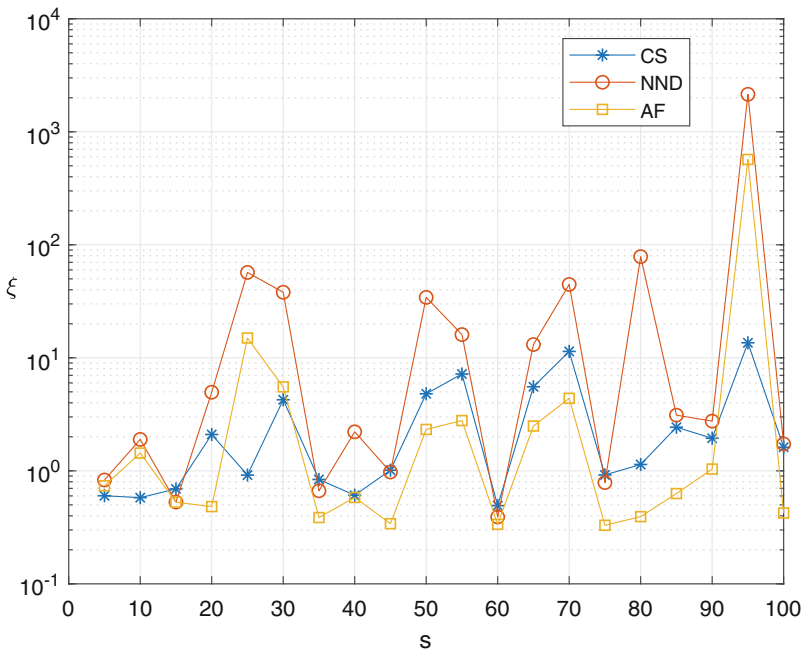


Fig. 1. ξ versus the number of event pulses s , $c = 1$, CS: compressed sensing, NND: nonnegative deconvolution, AF: adaptive filter

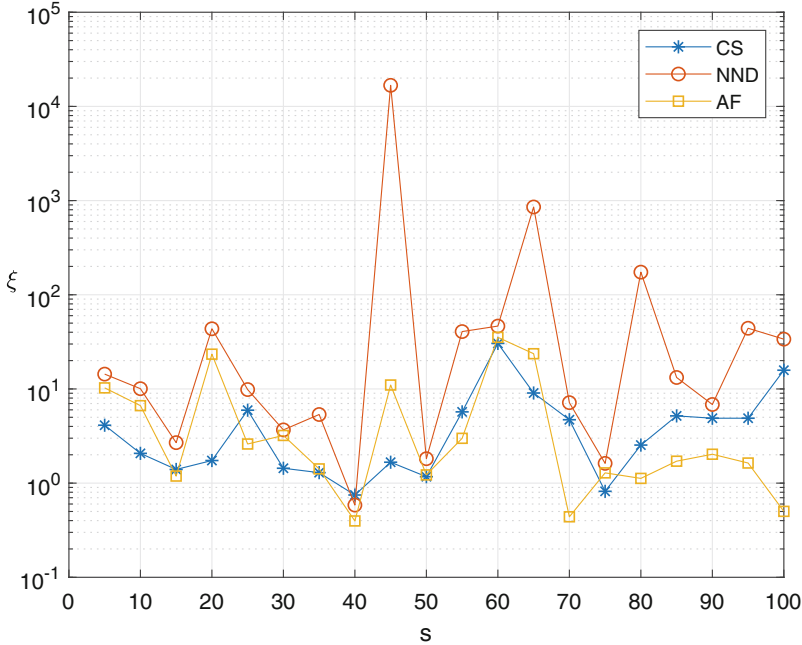


Fig. 2. ξ versus the number of event pulses s , $c = 5$, CS: compressed sensing, NND: nonnegative deconvolution, AF: adaptive filter

In Figs. 1, 2, 3 and 4, the average MSE versus the number of sparsity degree s of the SCR event signal \mathbf{x} is shown for the three compared algorithms:

- CS: the compressed sensing algorithm presented in [7];
- NND: the nonnegative deconvolution filtering technique described in [3];
- AF: the adaptive filter method proposed in this work.

The EDA synthetic signal has been generated by considering positive random values for the parameters τ_1, τ_2 with their means equal to respectively 10 and 1, while for the two algorithms that assume to know the information about the impulse response $h(n)$, i.e., CS and NND, $\tau_1 = 10$, and $\tau_2 = 1$. In this way, we have considered a sort of pulse shape variations that could better represent the real data behavior.

The performance of the proposed algorithm looks better, especially for lower values of c and higher ones for the sparsity degree s . It is important to note that since the synthetic model represents the main assumptions used by the CS algorithm, we think that this can justify why the CS algorithm performs better in some cases, especially for lower values of s . In the next section, we will consider a real data analysis in order to get more insights about the algorithm comparison.

5 Experimental Data Results

In order to test the described algorithm with real-world EDA signals, we have considered a video and reading stimuli experiment. In more details, the experi-

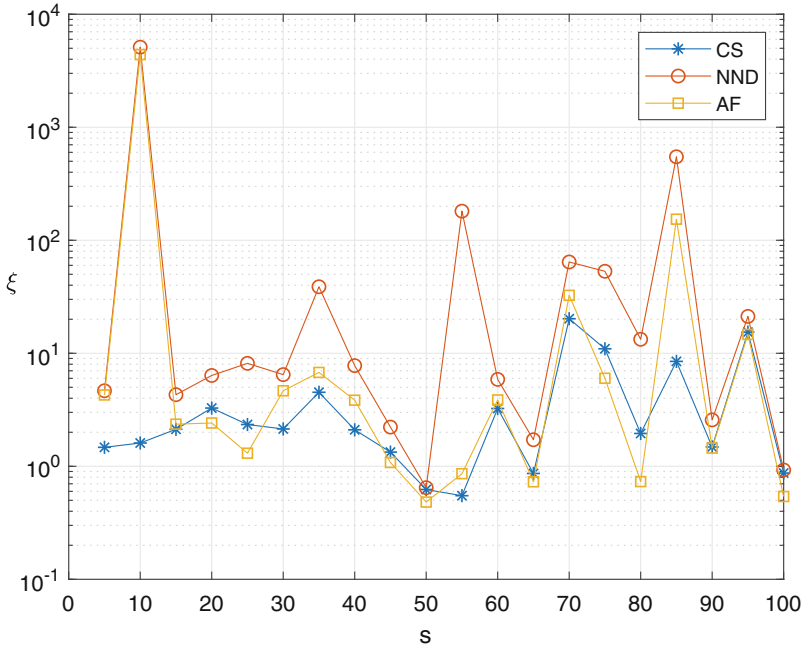


Fig. 3. ξ versus the number of event pulses s , $c = 10$, CS: compressed sensing, NND: nonnegative deconvolution, AF: adaptive filter

ment has been conducted in the three following step: a first neutral EDA measurement without stimuli, a second period of measurement with an erotic content video as stimulus, and, finally, the subjects under test were asked to read a brief erotic story.

5.1 Qualitative Results

As a first look at the experimental results, we consider the measured EDA signal, and the corresponding algorithm outputs, of one of the subjects participating to the experiment.

From Figs. 5, 6 and 7, it seems that the proposed adaptive filter solution produces an estimated event signal which is more sparse with respect to the estimates of the other two algorithms.

5.2 Quantitative Performance Evaluation

In order to verify if each of the two different non-neutral stimuli outputs a different EDA signal, we have counted the estimated number of SCR events by taking the mean of the obtained responses, for each subject under test.

In Fig. 8, it can be seen that all the three techniques are able to well discriminate the video stimulus from the others, for the four tested subjects. The

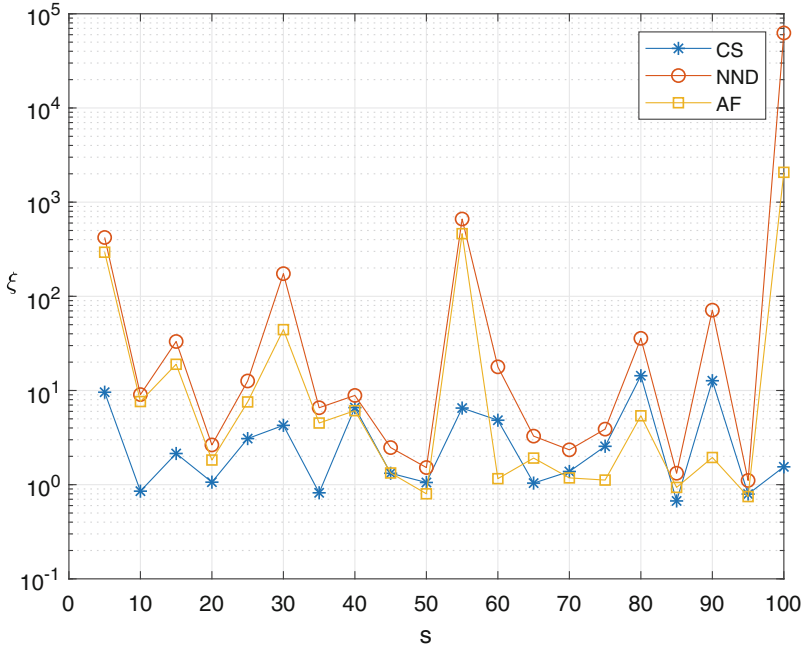


Fig. 4. ξ versus the number of event pulses s , $c = 20$, CS: compressed sensing, NND: nonnegative deconvolution, AF: adaptive filter

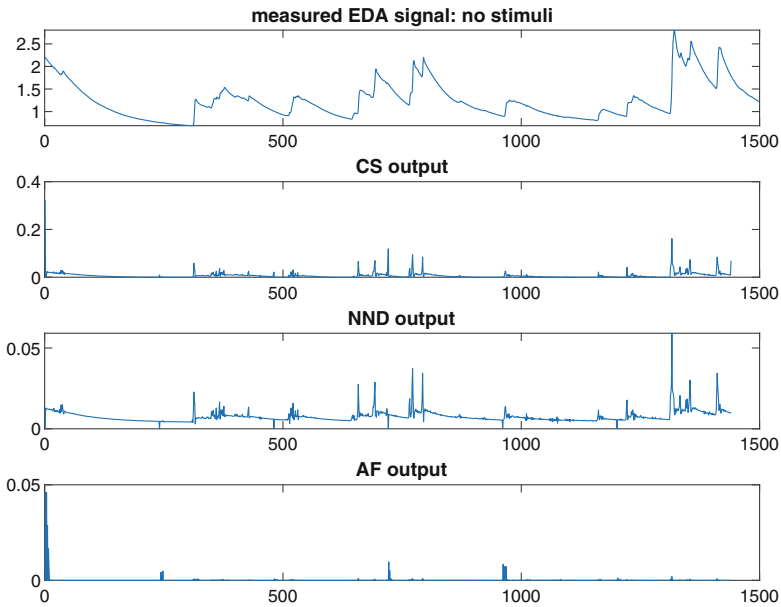


Fig. 5. Example of a subject measured and estimated responses without stimuli

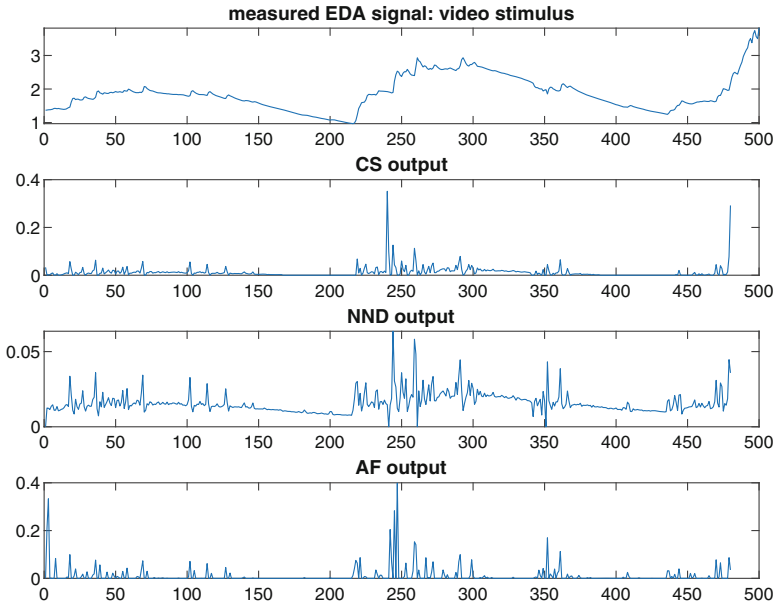


Fig. 6. Example of a subject measured and estimated responses with a video stimulus

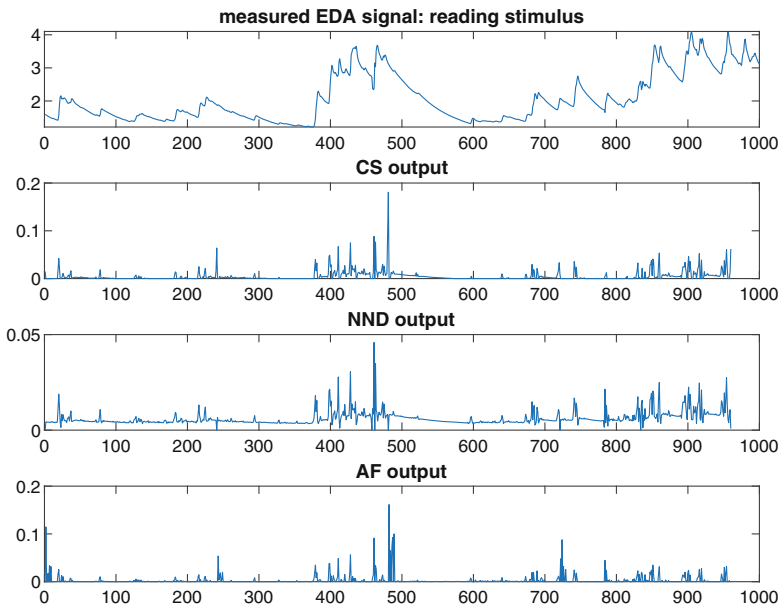


Fig. 7. Example of a subject measured and estimated responses with a reading stimulus

proposed techniques seems to be able to also address a difference between the neutral and reading stimulus.

Ongoing works will be devoted to better characterize this classification ability by considering alternative methods for counting the number of event pulses: as an example, a threshold with a more sophisticated method to count the number of pulses could provide more feasible results. Possible ways to face this problem may be derived from the spike signal processing literature [11].

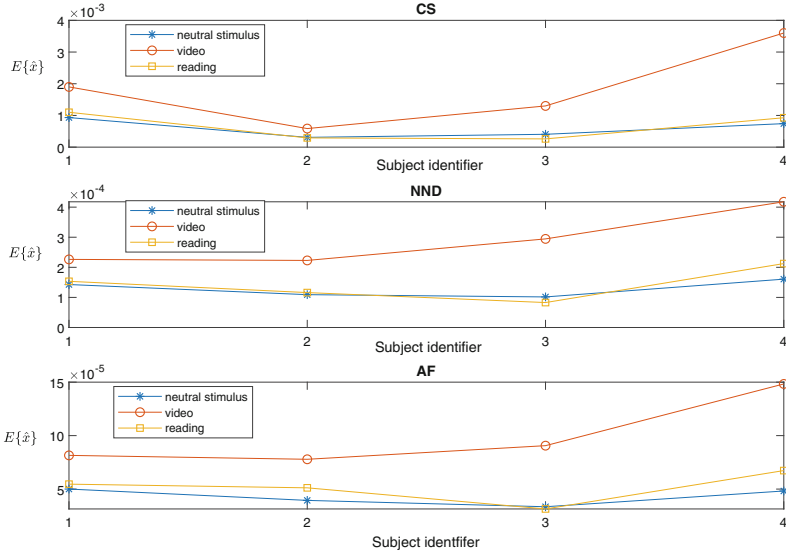


Fig. 8. Estimated SCR response mean per each subject

6 Conclusion

In this work, we have presented a novel method for estimating the SCR signal events through an adaptive filtering approach, which results independent on the impulse response parameters. The performance of the proposed approach has been proven by using both synthetic and experimental data.

Interesting perspective of future research lines may come from including the novel algorithm in a multi sensor wearable system, where the different measured outputs may be combined and processed, for instance, by a machine learning procedure in order to help medical diagnoses and therapies [12].

A further interesting development, from the area-body and intra-body networking point of view, could come from using intra-body communication systems, like [1,14], in order to optimize the collecting process of differently posed sensor measurements.

References

1. Banou, S., et al.: Beamforming galvanic coupling signals for IOMT implant-to-relay communication. *IEEE Sen. J.* 1 (2019). <https://doi.org/10.1109/JSEN.2018.2886561>
2. Benedek, M., Kaernbach, C.: A continuous measure of phasic electrodermal activity. *J. Neurosci. Methods* **190**(1), 80–91 (2010)
3. Benedek, M., Kaernbach, C.: Decomposition of skin conductance data by means of nonnegative deconvolution. *Psychophysiology* **47**(4), 647–658 (2010)
4. Boucsein, W.: *Electrodermal Activity*. Springer, New York (2012). <https://doi.org/10.1007/978-1-4614-1126-0>
5. Haykin, S.: *Adaptive Filter Theory*, 4th edn. Prentice Hall, Upper Saddle River (2002)
6. Hernando-Gallego, F., Luengo, D., Arts-Rodriguez, A.: Feature extraction of galvanic skin responses by nonnegative sparse deconvolution. *IEEE J. Biomed. Health Inform.* **22**(5), 1385–1394 (2018). <https://doi.org/10.1109/JBHI.2017.2780252>
7. Jain, S., Oswal, U., Xu, K.S., Eriksson, B., Haupt, J.: A compressed sensing based decomposition of electrodermal activity signals. *IEEE Trans. Biomed. Eng.* **64**(9), 2142–2151 (2017). <https://doi.org/10.1109/TBME.2016.2632523>
8. Kappas, A., Kster, D., Basedow, C., Dente, P.: A validation study of the affective q-sensor in different social laboratory situations (2013)
9. McCarthy, C., Pradhan, N., Redpath, C., Adler, A.: Validation of the empathica E4 wristband. In: 2016 IEEE EMBS International Student Conference (ISC), pp. 1–4, May 2016. <https://doi.org/10.1109/EMBSISC.2016.7508621>
10. Nishiyama, T., Sugeno, J., Matsumoto, T., Iwase, S., Mano, T.: Irregular activation of individual sweat glands in human sole observed by a videomicroscopy. *Auton. Neurosci.* **88**(1–2), 117–126 (2001)
11. Park, I.M., Seth, S., Paiva, A.R.C., Li, L., Principe, J.C.: Kernel methods on spike train space for neuroscience: a tutorial. *IEEE Signal Process. Mag.* **30**(4), 149–160 (2013). <https://doi.org/10.1109/MSP.2013.2251072>
12. Sano, A., et al.: Identifying objective physiological markers and modifiable behaviors for self-reported stress and mental health status using wearable sensors and mobile phones: observational study. *J. Med. Internet Res.* **20**(6), e210 (2018)
13. Sidis, B.: The nature and cause of the galvanic phenomenon. *J. Abnorm. Psychol.* **5**(2), 6974 (1910). <https://doi.org/10.1037/h0075352>
14. Swaminathan, M., Vizziello, A., Duong, D., Savazzi, P., Chowdhury, K.R.: Beamforming in the body: energy-efficient and collision-free communication for implants. In: IEEE INFOCOM 2017 - IEEE Conference on Computer Communications, pp. 1–9, May 2017. <https://doi.org/10.1109/INFOCOM.2017.8056989>
15. Wright, J.J., et al.: Toward an integrated continuum model of cerebral dynamics: the cerebral rhythms, synchronous oscillation and cortical stability. *BioSystems* **63**(1–3), 71–88 (2001)